

Article

Bio-Desilication of Coal Fly Ash and the Impacts on Critical Metal Recovery

Shulan Shi , Ting Chen, Simeng Ren and Jinhe Pan * 

Key Laboratory of Coal Processing & Efficient Utilization, Ministry of Education, School of Chemical Engineering and Technology, China University of Mining and Technology, Xuzhou 221116, China; slshi21@cumt.edu.cn (S.S.); cting@cumt.edu.cn (T.C.); ts24040245p31@cumt.edu.cn (S.R.)

* Correspondence: jinhepan@cumt.edu.cn

Abstract

Critical metals such as rare earth elements (REEs) are primarily associated with silicates and aluminosilicates in coal fly ash, resulting in poor REE recovery. Silicate bacteria can decompose silicate minerals and release silicon, but their impact on REE extraction remains unclear. In this study, two coal fly ash samples with different origins and combustion methods were bioleached by *Paenibacillus mucilaginosus*, and the effects of bio-desilication on REE leaching were examined. First, the optimal bio-desilication conditions were determined as a pulp density of 1%, an initial pH of 7.0 and an initial cell concentration $OD_{600} = 0.2$. Compared to circulating fluidized bed (CFB) coal fly ash, silicon in pulverized coal furnace (PCF) coal fly ash was more difficult to dissolve by *P. mucilaginosus*. After bio-desilication, the acid leaching rate of REEs improved by 8–15% for CFB coal fly ash but only 4–5% for the PCF sample. Further investigation found that the surface turned rough and the specific surface area of coal fly ash increased after bio-desilication, which are conducive to REE extraction. Additionally, there was more quartz and mullite in PCF coal fly ash, which are more resistant to biological corrosion than amorphous silicate. The results demonstrate that bio-desilication can improve REE recovery, providing new perspectives for the low-cost green utilization of coal fly ash.

Keywords: silicate bacteria; coal fly ash type; mineral phase; combustion method; green recovery



Academic Editor: Srecko Stopic

Received: 30 June 2025

Revised: 29 July 2025

Accepted: 6 August 2025

Published: 8 August 2025

Citation: Shi, S.; Chen, T.; Ren, S.; Pan, J. Bio-Desilication of Coal Fly Ash and the Impacts on Critical Metal Recovery. *Metals* **2025**, *15*, 891. <https://doi.org/10.3390/met15080891>

Copyright: © 2025 by the authors. Licensee MDPI, Basel, Switzerland. This article is an open access article distributed under the terms and conditions of the Creative Commons Attribution (CC BY) license (<https://creativecommons.org/licenses/by/4.0/>).

1. Introduction

Rare earth elements (REEs) are non-renewable national strategic resources. A coal combustion product, coal fly ash (CFA) is considered an unconventional REE resource, with vast reserves and an average REE concentration of ~500 ppm [1,2]. Extracting REEs from coal fly ash not only alleviates environmental pollution but also creates substantial economic value. Coal fly ash is mainly composed of Si, Al, Fe and Ca, which occur as amorphous silica, mullite, quartz, magnetite and hematite. In coal fly ash, REEs mainly exist in the forms of silicate and aluminosilicate [3]. Other fractions are REE oxides, phosphates and carbonates. According to the elemental composition, coal fly ash is classified into two types, C-type and F-type [4]. REEs are mainly associated with silicates and aluminosilicates in F-type fly ash, which causes difficulty for extraction. In contrast, 50–60% of REEs in C-type fly ash occur as carbonates and metal oxides [5], which are more readily extractable. Additionally, occurrence modes of REEs in CFA may also differ due to variations in origins and combustion methods [6], which affect the extractability of REEs. To date, physical

and chemical methods for extracting REEs from coal fly ash include thermal treatment, alkali treatment, acid leaching and solvent extraction [1,7,8]. Direct acid leaching exhibits a limited REE leaching rate, which is around 30–60% depending on coal fly ash type [1]. Pan et al. improved REE concentration through physical separation techniques (particle size, magnetic and density separation), then leached 79.85% REEs with 3 M HCl at 60 °C [7]. Around 88.15% of the total REEs were extracted from coal fly ash by 8 M HCl after NaOH hydrothermal treatment [9], because NaOH can dissolve aluminosilicate and release REE-bearing particles. Notably, NaOH roasting recovered more than 90% of the total REEs, outperforming other roasting additives, such as Na₂CO₃, CaO and Na₂O₂ [10]. Overall, alkaline roasting combined with acid leaching can achieve a high recovery rate of REEs, but it entails high chemical consumption and energy costs.

Bioleaching is a green metallurgy method characterized by low cost and environmental friendliness [11,12]. Through mineral/microbe interactions, metals are released from minerals [13]. Due to the high stability of silicates, direct bioleaching of coal fly ash usually exhibits poor performance [14,15]. Ma et al. reported that 30.91% REEs were bioleached by *Aspergillus niger*, which secreted oxalic acid, citric acid and acetic acid [15]. Alkaline pretreatment is employed to enhance REEs' recovery rate. For example, Fan et al. [16] roasted coal fly ash with Na₂CO₃, then 91.2% aluminum (Al) and 63.4% REEs were extracted by the bacteria *Acidithiobacillus ferrooxidans*. During Na₂CO₃ roasting mullite and sillimanite were transformed into more readily extractable nepheline. The bacteria *A. ferrooxidans* could oxidize pyrite and generate Fe³⁺ and H₂SO₄, resulting in dissolution of REEs. Also, Na₂CO₃ roasting promoted Ge, V and Li bioleaching from coal fly ash [17]. In that study, a spent-medium of *Pseudomonas putida* was utilized, which contained gluconic acid, oxalic acid and citric acid. In another case, *Acidithiobacillus thiooxidans* extracted approximately 80% of REEs from coal fly ash that had been pretreated via a hydrothermal-alkali method [18]. The hydrothermal-alkali treatment reduced the Si content of coal fly ash, and enhanced bacterial absorption to the fly ash particles. Although they enhance the bioleaching rate, alkali roasting or hydrothermal-alkali treatments require substantial alkali consumption and high temperature, thereby increasing the cost of REE recovery. Therefore, novel methods need to be investigated to break down the silicate and aluminosilicate structures of CFA without relying on alkaline pretreatment.

Silicate solubilizing bacteria or silicate bacteria are microorganisms capable of decomposing silicate minerals and releasing monosilicic acid. These bacteria are widely distributed in soil and plant rhizospheres, playing a key role in the silicon biogeochemical cycle, ecological systems and agricultural applications [19]. Numerous microorganisms can solubilize silicate minerals [20], such as *Bacillus*, *Paenibacillus*, *Pseudomonas* and *Acidithiobacillus*. Silicate bacteria have been utilized for bio-beneficiation. For instance, the ratio of Al₂O₃/SiO₂ in bauxite was improved following bio-desilication by *Burkholderia anthina* [21]. Some silicate bacteria have been successfully applied to process coal fly ash. Sen et al. reported a 22% reduction in silica content of coal fly ash after 60 days of bioleaching with *Bacillus barbaricus* [22], while alumina content increased by 9%. Another effective species for bio-desilication of coal fly ash is *Bacillus amyloliquefaciens* [23]. In the leachate, Si concentration reached 306.26 mg/L, while Al concentration was only 0.5 mg/L. These results demonstrate that silicate bacteria could be applied to selectively leach silicon and concentrate metals in coal fly ash. However, the impact of bio-desilication on leachability of rare earth elements from coal fly ash remains unknown.

Paenibacillus mucilaginosus is a kind of typical silicate bacterium and can release silicon, phosphorus and potassium from silicate minerals (e.g., feldspar and mica) by producing organic acids, exopolysaccharide and siderophore [24,25]. Thus, it functions as biofertilizer in agriculture to promote plant growth [26]. Additionally, it has been utilized to extract

Si, Li and V from silicate minerals such as lepidolite [27], bauxite [28], stone coal and coal tailing [29]. For instance, *P. mucilaginosus* was found to convert insoluble silicon in coal tailings into bioavailable silicon, and leached 260 mg/L silicon after 16 days [29]. Oxalic acid, tartaric acid, citric acid and malic acid secreted by bacteria are primary factors contributing to silicon leaching. These organic acids decompose minerals, thereby releasing inorganic nutrients from coal fly ash. Moreover, the bacteria synthesize more extracellular polysaccharide in response to mineral-induced stress [24]. Notably, coal fly ash constitutes an oligotrophic environment for microorganisms, necessitating an external nitrogen source. *P. mucilaginosus* is capable of nitrogen fixation, which reduces the cost of bio-desilication of CFA. The bacterium can utilize diverse carbon sources [30], and is easily obtained and cultivated. Overall, *P. mucilaginosus* shows great potential for desilication of coal fly ash.

Direct acid leaching of coal fly ash exhibits poor REE recovery. Silicate bacteria can destroy the structure of silicates, but their influence on REE leachability remains unexplored. In this study, to enhance the acid leaching rate of REEs while reducing costs, *P. mucilaginosus* was employed to leach silicon from different types of coal fly ash. The bioleaching conditions were optimized and the impact of bio-desilication on REE extractability was explored. Furthermore, the underlying mechanisms were elucidated. This study provides fundamental insights into the relationship between Si and REE extraction, which will lower the cost of REE recovery and facilitate green utilization of coal fly ash.

2. Materials and Methods

2.1. Materials

Coal fly ash samples were collected from Zhunneng power station, Jungar, Inner Mongolia, China, and Faer power station, Liupanshui, Guizhou, China. The Jungar coal fly ash was generated from circulating fluidized bed (CFB), while the Faer coal fly ash was produced by pulverized coal furnace (PCF). The elemental composition of the two CFA samples was analyzed in a previous study [6]. They are mainly composed of SiO_2 and Al_2O_3 . Compared to CFB CFA, there is more SiO_2 and less Al_2O_3 in PCF CFA. PCF CFA also has more Fe_2O_3 (12.1%) than CFB CFA (2.59%). For both coal fly ash samples, the CaO content is lower than 10%, so they are F-type coal fly ash. The total rare earth element content is 516.80 ppm and 520.27 ppm for CFB and PCF CFA, respectively [6]. La, Ce, Pr, Nd and Y are the main rare earth elements in the two CFA samples. The silicate bacterium strain *Paenibacillus mucilaginosus* was obtained from Guangdong Microbial Culture Collection Center, with GDMCC No. 1.15. It was cultured in shake flasks at 30 °C, 170 rpm with initial pH 6.8. Culture medium A [31] is composed of 10.0 g/L sucrose, 2.0 g/L K_2HPO_4 , 0.5 g/L MgSO_4 , 0.5 g/L yeast extract, 1.0 g/L $(\text{NH}_4)_2\text{SO}_4$, 0.1 g/L NaCl and 0.1 g/L CaCO_3 . Culture medium B is a selective medium for silicate bacteria, containing 5.0 g/L sucrose, 2.0 g/L Na_2HPO_4 , 0.5 g/L $\text{MgSO}_4 \cdot 7\text{H}_2\text{O}$, 0.005 g/L FeCl_3 and 0.1 g/L CaCO_3 [32].

2.2. Bio-Desilication of Coal Fly Ash

The coal fly ash samples were dried at 105 °C for 8 h before the bioleaching experiments. Culture medium A containing coal fly ash was sterilized at 121 °C for 20 min. Then, *P. mucilaginosus* was added to the shake flask. The bioleaching experiments were conducted in a horizontal shaker at 170 rpm and 30 °C for 8 days. Pulp density, initial pH and initial cell concentration were optimized by single factor experiment. Five pulp densities were tested, including 1%, 2%, 4%, 6% and 8% (*w/v*). Initial cell optical density at 600 nm (OD_{600}) was set at 0.10, 0.20, 0.40, 1.00 and 2.00. Groups without bacteria were set as abiotic controls. Six initial pH values (4.00, 5.00, 6.00, 7.00, 8.00, 9.00) were tested. Moreover, bio-desilication under different culture media and for different CFA types was also explored. The impact of culture medium on bio-desilication of Jungar CFA was explored at 2% pulp density,

initial pH 6 and initial cell OD₆₀₀ 0.20. The impact of coal fly ash type on bio-desilication was explored with culture medium A, 2% pulp density, initial pH 6 and initial cell OD₆₀₀ 0.20. Optical density at 600 nm (OD₆₀₀) was used to characterize cell concentration, and was measured by a cell density meter (Ultrospec 10, Biochrom, Cambridge, UK, ± 0.01). The pH value of leachate was monitored every day with a pH meter (PHSJ-3F, Leici, Shanghai, China, ± 0.01). Supernatant was collected by centrifugation at 8000 rpm for 10 min. Si concentration in leachate was measured by the silicon molybdenum blue spectrophotometry method with RSD 0.3% [33]. We added the leachate to 0.10 mol/L hydrochloric acid system. Ethanol and ammonium molybdate were added to form silicon molybdenum yellow. Then, an oxalic acid/sulfuric acid mixture was added to eliminate the interference of impurities (P and As). Ammonium ferrous sulfate was added to reduce silicon molybdenum yellow to silicon molybdenum blue. The absorbance of the solution at 680 nm was measured with an ultraviolet/visible spectrophotometer (PERSEE TU-1901, Beijing, China). The concentration of organic acids in the leachate was detected by high-performance liquid chromatography (HPLC Agilent1260 infinity II, Santa Clara, CA, USA) using a C18 column (Neptune 5u, FLM, Guangzhou, China) (RSD 1%). The mobile phase was 0.5% KH₂PO₄ and 5% acetonitrile in water, with a flow rate of 0.5 mL/min at 30 °C. Each experiment was performed in triplicate.

2.3. Acid Leaching of Rare Earth Elements

After bio-desilication, residue CFA was collected by centrifugation at 8000 rpm for 10 min, and subjected to acid leaching at 60 °C for 2 h, with the following conditions: 200 rpm and 2% (*w/v*) pulp density. Three HCl concentrations (1 mol/L, 2 mol/L and 3 mol/L) were tested. REE concentration in leachate was measured by inductively coupled plasma mass spectrometry (Agilent 7900 ICP-MS, Santa Clara, CA, USA) with RSD 2%. The X-ray diffraction (XRD) patterns of the coal fly ash were recorded on a D8 ADVANCE diffractometer (Bruker, Karlsruhe, Germany) over 4–70°. Scanning electron microscopy (SEM; VEGA Compact, Tescan, Brno, Czech) was utilized to characterize the surface morphology of the coal fly ash. Functional groups on the surface of coal fly ash were analyzed using a Fourier transform infrared (FTIR) spectrometer (VERTEX 80V Bruker, Karlsruhe, Germany), with a scanning range of 4000–400 cm^{−1} and resolution of 4 cm^{−1}. The specific surface area of the coal fly ash was determined by nitrogen absorption/desorption analysis (Autosorb-iQ, Quantachrome, Boynton Beach, FL, USA). Next, 0.5 g coal fly ash was degassed in a vacuum drying oven at 60 °C for 2 h. The nitrogen adsorption was measured in a relative pressure range of 0.05–0.30 at 77.350 K. The specific surface area was calculated based on BET theory with correlation coefficient >0.999 (RSD 3%). All data were processed and visualized using Excel 2019 and Origin 9.0 software. Statistical differences across leaching rates of different groups were analyzed by analysis of variance (ANOVA) with IBM SPSS Statistics 19.

3. Results and Discussion

3.1. Bio-Desilication of Coal Fly Ash by *P. mucilaginosus*

3.1.1. Condition Optimization of Bio-Desilication

Bioleaching performances of microorganisms are largely affected by leaching conditions. Pulp density, initial cell concentration and initial pH were optimized in this study. The results showed that pulp density of coal fly ash affects Si bioleaching significantly. The Si concentration in leachate peaked on days 3–5, depending on the pulp density (Figure 1A). For the 2% pulp density group, the Si concentration peaked on day 5, then remained almost unchanged on days 6 and 7, and decreased on day 8. The decrease in Si concentration is probably due to the adsorption of Si onto polysaccharides produced by

the bacteria [31]. The leaching system is viscous, indicating the production of extracellular polymeric substances. For the 8% pulp density group, the Si concentration peaked on day 3, then decreased from day 4 to day 8. Generally, the Si concentration in leachate increased with the increase in pulp density. In the 1% pulp density group, the maximum Si concentration was 64 ppm. In the 6% pulp density group, the Si concentration reached a maximum of 119 ppm. A further increase in pulp density (8%) led to a decrease in Si concentration.

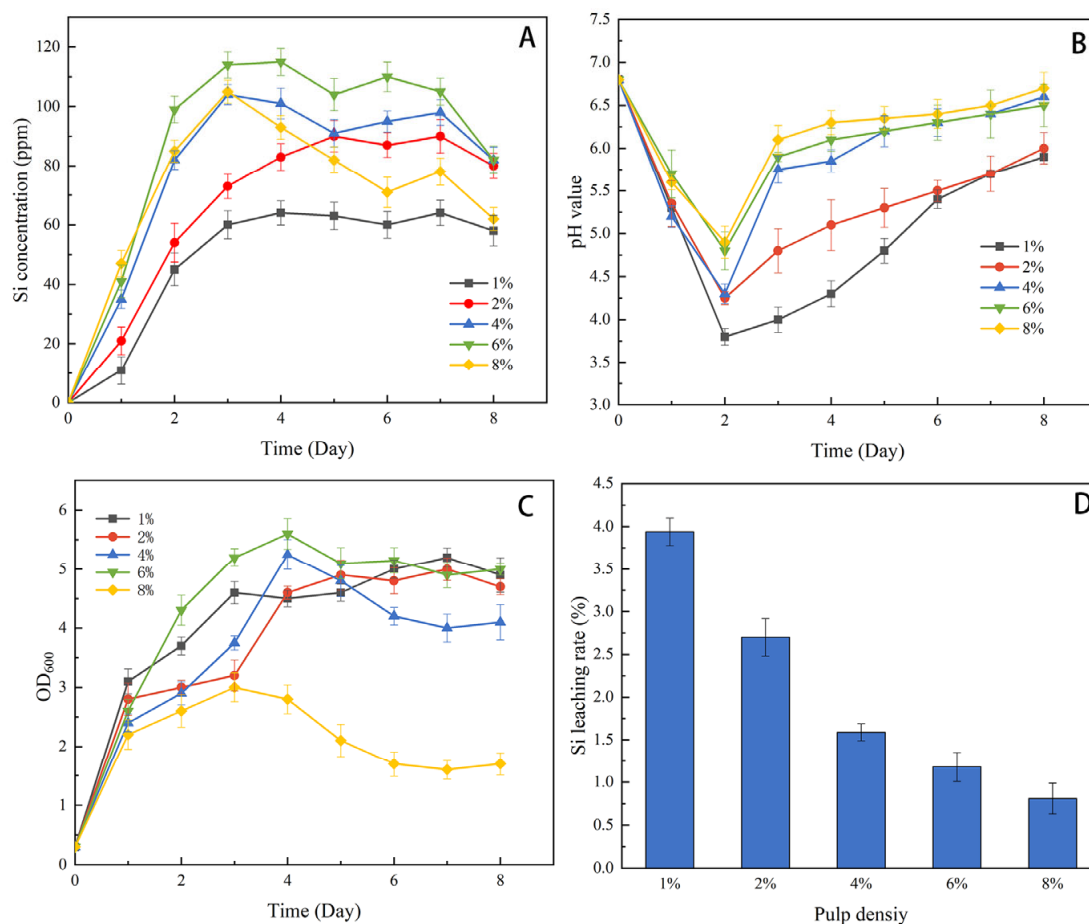


Figure 1. Si concentration (A), pH value (B), bacterial concentration (C) and Si leaching rate (D) in bioleaching system with different pulp densities.

The metabolism of bacteria is attributed to a reduction in pH. The pH of the leaching system was lowest in the 1% pulp density group and highest in the 8% pulp density group (Figure 1B). The pH decreased from 6.8 to 5.0, or even to 3.8 during the first two days, then increased gradually in all experimental groups. The pH rose more rapidly in high pulp density (4%, 6%, 8%) groups. On day 8, the pH reached 6.0–6.5, slightly lower than the initial pH. The 1% and 2% pulp density groups showed a lower pH value than the other groups on day 8. This result indicated that organic acids were produced by *P. mucilaginosus*. Guo et al. reported that organic acid is the main reason for Si dissolution [23]. H^+ adsorbs onto the silicate surface, resulting in the polarization of Si-O bonds and release of silicon from minerals. Meanwhile, organic acid radicals (e.g., oxalate) nucleophilically attack silica, promoting breakage of Si-O bonds [34]. Then, organic acids are gradually consumed, and the bacteria produces fewer organic acids during the stationary and decline phases, both leading to the increase in pH in the middle and late periods of bioleaching. For the 8% pulp density group, fewer organic acids were produced and more coal fly ash consumed organic acids, so its pH was the highest among all groups.

Both Si concentration and pH of bioleaching systems are closely related to bacterial growth. Cell concentration increased at the early stage of bioleaching in all experimental groups, showing that *P. mucilaginosus* can adapt to the environment and is suitable for bio-desilication of coal fly ash. In the 1% and 2% pulp density groups, the cell concentration increased during the first 3–4 days, and remained constant (OD_{600} 4.6–4.9) later (Figure 1C). In the 4% and 6% pulp density groups, the cell concentration decreased after day 4. The reason is that with the consumption of nutrients, bacteria may die or form spores. The cell concentration in the 4% and 6% pulp density groups was higher than that in the 1% and 2% pulp density groups on day 4. On day 8, the cell concentration was similar in the 1%, 2% and 6% pulp density groups, higher than in the 4% pulp density group. In the 8% pulp density group, cell concentration was the lowest and decreased earlier than the other groups, suggesting the toxicity of large amounts of coal fly ash to *P. mucilaginosus* [35]. Coal fly ash contains harmful heavy metals, such as Cr, Mn, Co and Ni. During bioleaching, the release of these heavy metals probably exerts stress on bacterial growth. Higher pulp density represents higher toxicity; thus, cell concentration was lower and fewer organic acids were produced, leading to a lower Si leaching rate. Moreover, high pulp densities may impair bioleaching efficiency by limiting bacterial access to essential nutrients and oxygen due to constrained mass transfer conditions.

With the increase in pulp density, the Si leaching rate decreased from 3.94% to 0.8% (Figure 1D). The highest Si leaching rate was observed in the 1% pulp density group, although the 6% pulp density group showed the highest Si concentration. This is because more cells and metabolites could react with coal fly ash under low pulp density [16]. *P. mucilaginosus* was utilized to process coal fly ash in another study. With 50% pulp density and higher inoculation, the Si concentration in leachate reached 1020.68 mg/L but the Si leaching rate was only 0.7% [36]. This is because high pulp density poses challenges to the growth and metabolism of bacteria. Consistently, the 8% pulp density group exhibited the lowest cell concentration and the highest pH, demonstrating that large amounts of coal fly ash inhibited the growth and organic acid production of *P. mucilaginosus*. To summarize, 1% is optimal pulp density for bio-desilication, and a further decrease in pulp density would increase the cost.

Five initial cell concentrations (OD_{600} = 0.1, 0.2, 1, 2, 4) were set to explore the influence of inoculation amounts of bacteria on the Si leaching rate. Generally, the influence of inoculum size on bio-desilication was less than pulp density, and the Si concentration did not vary much among groups. The results showed that the Si leaching rate increased first and then decreased with the increase in the inoculum size of *P. mucilaginosus* (Figure 2A). In the abiotic control group, the Si concentration was significantly lower, and the pH was higher compared to the experimental groups, proving that bacteria contribute to desilication. The highest Si leaching rate was achieved at OD_{600} = 0.2, followed by the OD_{600} = 1 group. The groups with OD_{600} = 0.4, 1.0 and 2.0 showed a lower pH value compared to the other experimental groups during the first three days, but the pH value was similar among all experimental groups on day 8 (Figure 2B). When the inoculation amount is very low, the adaptation of bacteria to the leaching environment decreases and the interaction between bacteria and coal fly ash is weak [37]. In the lowest inoculum group (OD_{600} = 0.1), the pH decreased slowly at the early stage of bioleaching, and Si concentration increased slowly. Consequently, fewer organic acids were generated and less silicon was released. When the inoculation amount was very high, nutrients in the culture medium were consumed quickly and competition between cells increased, which is disadvantageous to the dissolution of Si. In the high inoculum (OD_{600} = 2) group, the pH was lower than the other groups at the early stage, indicating rapid metabolism. Then

its pH value increased and Si concentration decreased earlier than the other groups. The optimal initial cell concentration is $OD_{600} = 0.2$.

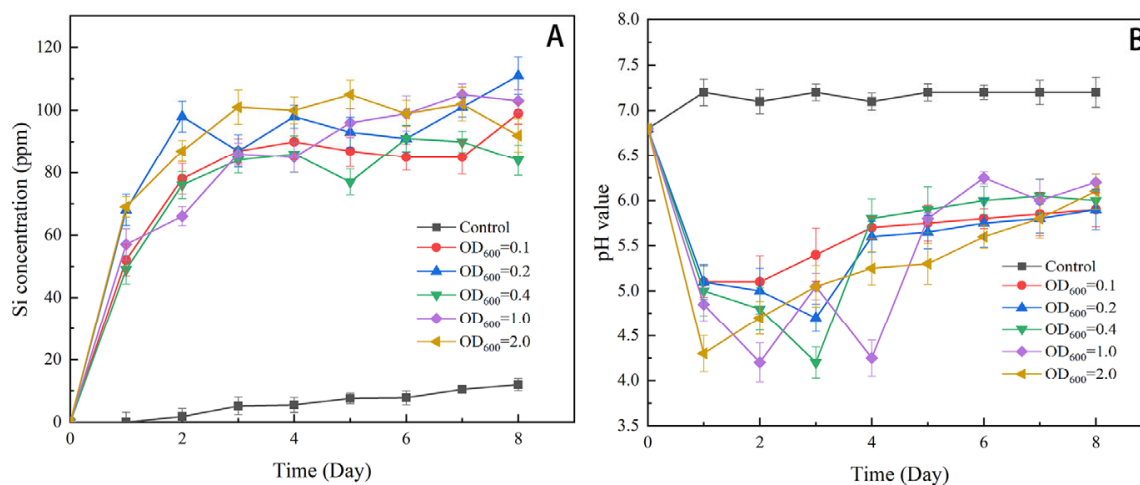


Figure 2. Si concentration (A) and pH value (B) in bioleaching systems with different bacterial inocula.

Initial pH is also an essential factor affecting bacterial growth and desilication. In this study, the Si leaching rate of different initial pH groups (from 4 to 9) was compared. The Si concentration was highest in the pH 4 group, followed by the pH 5 group, and lowest in the pH 9 group (Figure 3A), demonstrating that low pH favors the dissolution of silicon. The Si concentration increased slowly and decreased after day 6 in the pH 9 group. In the other groups, the Si concentration increased rapidly and then remained constant. During bioleaching, the pH decreased first due to metabolism of *P. mucilaginosus*, and increased gradually in all groups. The pH was relatively high in the pH 9 and pH 8 groups, followed by the pH 6 and 7 groups, and lowest in the pH 4 and pH 5 groups (Figure 3B). The cell concentration increased in all groups, indicating that *P. mucilaginosus* can adapt to a wide range of pH (Figure 3C). The bacterial amount was higher in the pH 7 and pH 8 groups than the other groups. The Si leaching rate decreased with the increase in initial pH within the pH range of 4–6, and remained almost unchanged between pH 6 and pH 8 (Figure 3D). The Si leaching rate was lowest at pH 9, because *P. mucilaginosus* struggles to survive in a very alkaline environment and little organic acid is secreted. The highest Si leaching rate was achieved at an initial pH of 4. Similarly, the Si concentration in the abiotic control group also increased with the increase in initial pH, suggesting that it is H_2SO_4 in the culture medium causing a high Si leaching rate rather than the function of *P. mucilaginosus*. Excluding the impact of H_2SO_4 , the Si leaching rate is similar in groups with an initial pH of 4–8. Considering that adding acid or alkali will increase the cost of bio-desilication, pH 7 was recommended as the optimal initial pH. In summary, Si bioleaching conditions were optimized as pulp density 1%, initial cell concentration $OD_{600} = 0.2$ and initial pH 7. The maximum Si leaching rate is 3.94%, which is low compared to alkali desilication but comparable to bio-desilication in other studies [38]. The low leaching rate is due to the limited leaching time, and a longer duration of bioleaching may increase the Si leaching rate further.

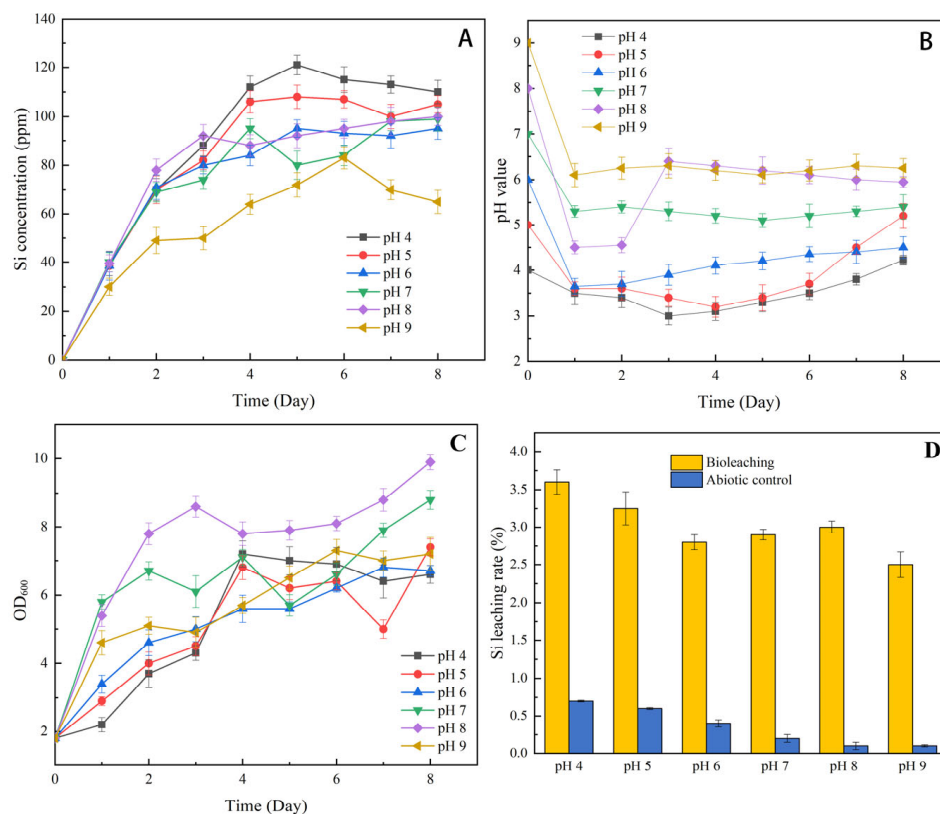


Figure 3. Si concentration (A), pH (B), bacterial concentration (C) and Si leaching rate (D) in bioleaching system with different initial pH.

3.1.2. The Effect of Culture Medium on Desilication

The composition of a culture medium significantly affects the growth and metabolism of microorganisms. Two commonly used culture media for silicate bacteria were compared in this study. Compared to culture medium B, medium A contains a nitrogen source and a higher concentration of carbon source (sucrose). Culture medium A exhibits a higher Si leaching rate than medium B in the short term but a similar leaching rate in the long term (Figure 4). The pH value of culture medium A was lower than that of medium B, and the pH decreased more rapidly in culture medium A, indicating that more organic acids were produced by *P. mucilaginosus* when the carbon source was abundant [39]. The results are confirmed by HPLC analyses. Tartaric acid (0.53 g/L), citric acid (1.75 g/L) and oxalic acid (0.36 g/L) were produced by bacteria in culture medium A. More tartaric acid but less citric and oxalic acid were detected in culture medium B (Table 1).

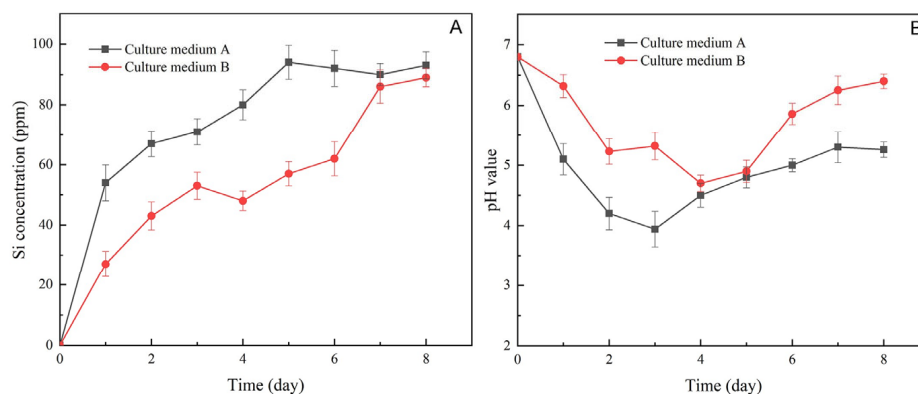


Figure 4. Si concentration (A) and pH value (B) in different culture media.

Table 1. Organic acids concentration (g/L) in bioleaching systems with different culture media.

	Tartaric Acid	Citric Acid	Oxalic Acid
Culture medium A	0.53	1.75	0.36
Culture medium B	1.61	0.09	0.14

Sucrose is the main substrate for organic acid synthesis. There was more sucrose in culture medium A, so more organic acids were produced. The two culture media also differed in nitrogen source. $(\text{NH}_4)_2\text{SO}_4$ served as the nitrogen source in culture medium A, whereas culture medium B lacked a nitrogen source, requiring *P. mucilaginosus* to perform nitrogen fixation. Nitrogen fixation reduces the bacterial growth rate [40], which has a negative effect on bio-desilication. Moreover, yeast extract in culture medium A is also beneficial for exopolysaccharide production of *Paenibacillus* [39]. Exopolysaccharide contains functional groups such as -OH, -COO- and $-\text{NH}_2\text{COCH}_3$, which react with Si in coal fly ash. This might be a reason for the high desilication performance of culture medium A, but further verification is needed. Additionally, Fe^{3+} in culture medium B hinders Si dissolution from silicate [34]. Overall, culture medium A is suitable for bio-desilication.

Culture medium B showed a similar Si concentration to culture medium A during the late stage of bioleaching, suggesting that effective desilication can be achieved under nutrient-limited conditions, albeit requiring more time. With low cost, culture medium B showed markedly greater potential for practical applications. Moreover, without a nitrogen source, culture medium B is selective to silicate bacteria, so it is difficult for it to be contaminated by other microorganisms. In the future, to decrease the cost, more economical carbon sources should be explored, such as molasses.

3.1.3. The Effect of Coal Fly Ash Type on Desilication

Silicate minerals possess diverse structures, such as layered, island, chained and framed, which are different in stability. Whether a silicate is easily or recalcitrantly decomposed by microorganisms depends largely on its structure [41]. For example, mullite is more readily decomposed by silicate bacteria than quartz in coal fly ash [22]. Therefore, the structure of silicate minerals directly influences Si leaching. The composition and structure of coal fly ash vary owing to feed coal properties and combustion conditions. In this study, the bio-desilication of two kinds of coal fly ash was compared. In the CFB CFA group, the Si concentration in leachate increased rapidly until day 5, then decreased slightly (Figure 5A). In the PCF CFA group, the Si concentration increased gradually, and remained constant during the last three days. The Si concentration in the CFB CFA group peaked on day 5 (102 ppm), whereas the maximum Si concentration in the PCF CFA group was (58 ppm). CFB CFA showed a higher Si leaching rate than PCF coal fly ash, which was 4.32% and 1.24%, respectively. This demonstrated that silicon in PCF coal fly was more difficult to dissolve. The pH curve was similar between the two groups, which declined during the first three days and subsequently increased (Figure 5B). The pH in the CFB CFA group decreased more quickly in the early stage, and increased more quickly than that in the PCF CFA group after day 4. The lowest pH was around 4.5 in both groups, indicating that the amount of organic acids generated by *P. mucilaginosus* was comparable in both groups. The divergent Si leaching rate is mainly due to the intrinsic properties of coal fly ash.

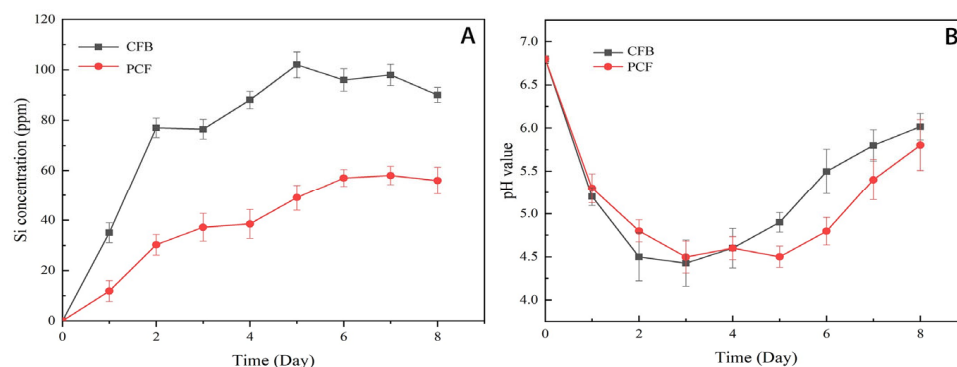


Figure 5. Si concentration (A) and pH (B) in bioleaching systems of circulating fluidized bed (CFB) and pulverized coal furnace (PCF) coal fly ash.

3.2. The Effect of Bio-Desilication on REE Extraction

REEs exist mainly in the forms of silicate and aluminosilicate in coal fly ash, which are resistant to acid corrosion. Direct acid leaching therefore exhibits poor REE recovery efficiency. Silicate bacteria can destroy the structure of these silicates, which is in favor of REE extraction theoretically. However, the influence of bio-desilication on REE leachability remains unexplored. In this study, *P. mucilaginosus* was employed to remove Si from CFB and PCF coal fly ash. After bio-desilication, CFA residues were subjected to hydrochloric acid leaching. Under 1 M, 2 M and 3 M HCl, the REE leaching rate was 41–47% for raw CFB CFA and only 9–12% for raw PCF CFA (Figure 6), demonstrating that REEs in CFB coal fly ash were more readily extracted by acid. This is because there are more aluminosilicate REEs in PCF than in CFB coal fly ash, and less organic/sulfide and acid soluble REEs [6]. The acid leaching rate of REEs increased with rising HCl concentration, consistent with previous studies [7]. In particular, the REE acid leaching rate increased significantly ($p < 0.01$) after bio-desilication for both CFA samples (Figures 6 and S1). Under 1 M, 2 M and 3 M HCl, the REE leaching rates of CFB coal fly ash residue were 49.63%, 55.24% and 62.54%, respectively, which increased by 8.38–15.28% compared to raw coal fly ash. In particular, the La recovery rate from CFB coal fly ash residue reached 82.58%, and the Ce and Pr recovery rates were around 70% in the 3 M HCl group (Figure 7). The Nd, Sm and Gd recovery rates ranged from 40% to 60%, whereas other REEs showed a recovery rate $< 40\%$. Most of the rare earth elements exhibited a higher leaching rate in CFB coal fly ash residues than the raw samples, except for Tm and Lu. By contrast, the REE leaching rate of PCF coal fly ash residue increased by merely 4.42–5.43% compared to raw PCF coal fly ash, significantly lower than the increment of the CFB samples. In the 3 M HCl group, the Sm recovery rate from PCF coal fly ash residue reached 18.07%, followed by Gd, Tb and Nd. The recovery rates of Ho, Er, Tm and Lu were $< 14\%$. All the rare earth elements exhibited a higher leaching rate in PCF coal fly ash residues than the raw samples. Considering the RSD of inductively coupled plasma mass spectrometry is 2%, the improvement of leaching rates possibly derives from the measurement errors.

The results illustrated that bio-desilication can improve the REE acid leaching of both CFA samples. Most REEs in coal fly ash are associated with aluminosilicate. The decomposition of aluminosilicate by silicate bacteria facilitates REEs dissolution. Furthermore, the REE acid leaching rate of CFB CFA was enhanced more significantly than that of PCF CFA (Figure 6). A possible reason is that more Si-O-Si (Al) bonds in CFB CFA were broken by bacteria, thus exposing more REEs to react with HCl. Consequently, the REE acid leaching rate increased more significantly than for PCF CFA. *P. mucilaginosus* has been used to activate coal fly ash in previous studies. For example, after desilication by *P. mucilaginosus*, surface Ca and Al contents increased [36], and the alkali leaching rates of Al and Si in

coal fly ash were improved [42]. These findings indicate that the physical and chemical properties of coal fly ash are altered by silicate bacteria, and the underlying mechanisms need to be investigated further.

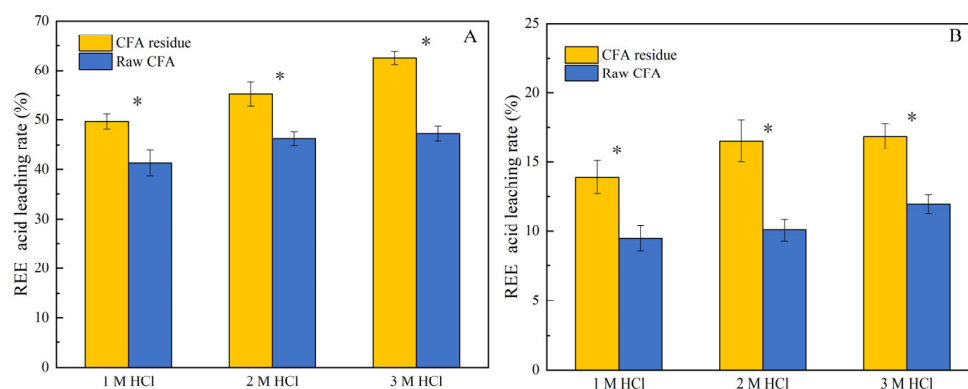


Figure 6. REE acid leaching rate of circulating fluidized bed coal fly ash (A) and pulverized coal furnace coal fly ash (B). Significant differences ($p < 0.01$) are labeled with *.

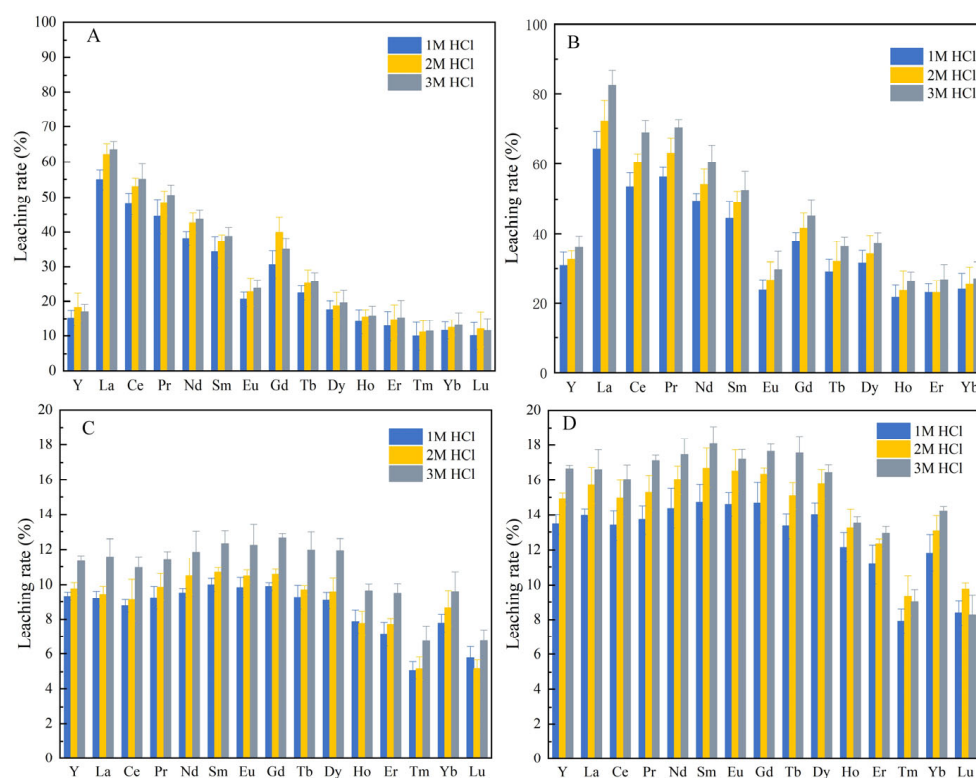


Figure 7. Acid leaching rate of single rare earth elements of raw CFB coal fly ash (A), CFB coal fly ash residue (B), raw PCF coal fly ash (C) and PCF coal fly ash residue (D). CFB, circulating fluidized bed; PCF, pulverized coal furnace.

3.3. Bio-Desilication Mechanisms

To elucidate the impact mechanism of bio-desilication regarding REE extraction, the surface morphology of coal fly ash before and after bioleaching was observed via SEM. Raw PCF CFA was spherical with a smooth surface (Figure 8), which is because silicate minerals in coal melt under elevated temperatures (1000–1200 °C). During bioleaching, *P. mucilaginosus* cells adhered to the CFA surface, and secreted organic acids (oxalic acid, citric acid and lactic acid) and polysaccharides, resulting in erosion and even breakdown of CFA. Therefore, etch pits and fragments could be observed on the PCF CFA residue. The findings

align with a previous study, in which surface properties of CFA were changed during bio-desilication, including a rougher surface and lower surface Si/Al ratio [36]. Bacterial etching exposed encapsulated REEs to acid attack, thereby promoting REE extraction.

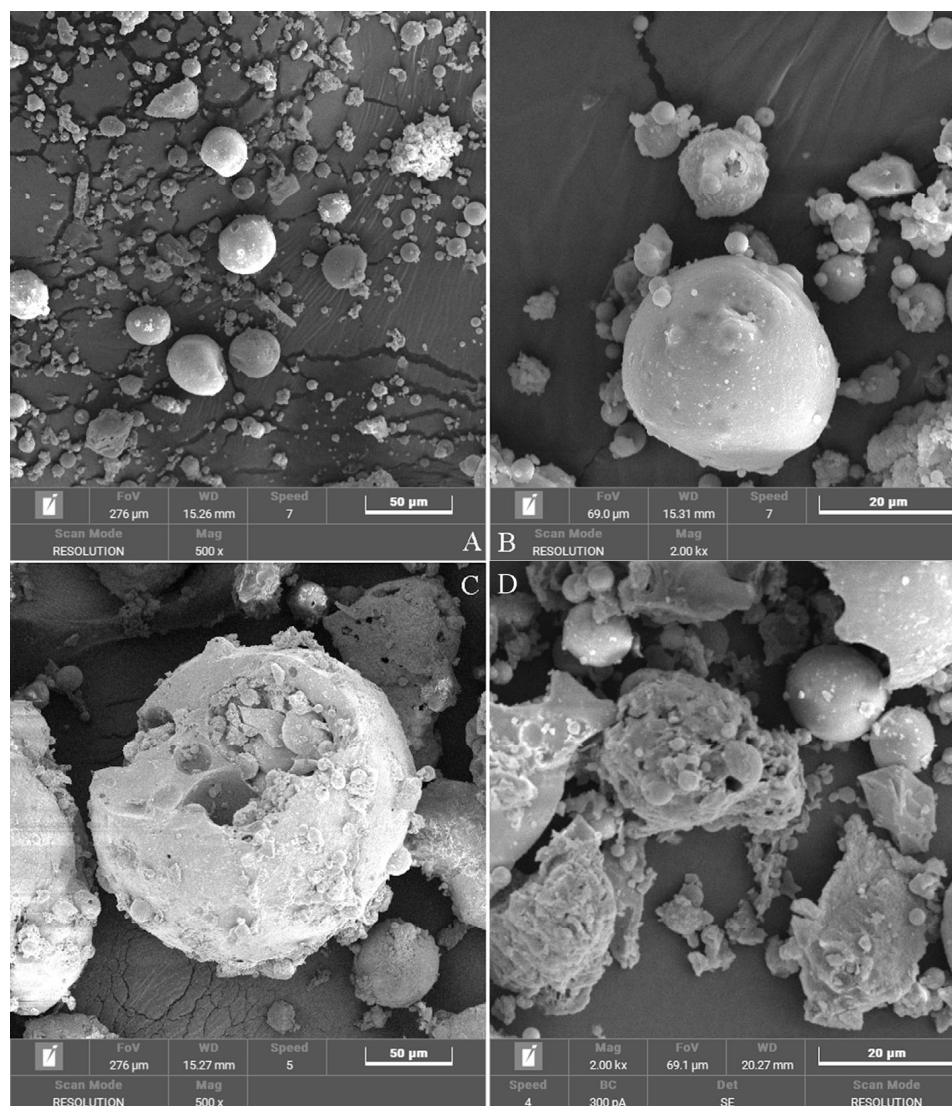


Figure 8. SEM of pulverized coal furnace coal fly ash before (A,B) and after bioleaching (C,D).

As for raw CFB CFA, it showed an irregular shape and a rough surface (Figure 9), representing typical characteristics of CFA from circulating fluidized bed. The rough surface renders it more easily absorbed and decomposed by *P. mucilaginosus*. Consequently, silicon was more readily dissolved from CFB coal fly ash compared to PCF samples. After bio-desilication, the particles fragmented and the particle size decreased. Furthermore, the surface changes of CFB coal fly ash were verified by FTIR (Figure 10). After bio-desilication, the absorbance of Si-O-Si/Al (1100 and 822 cm^{-1}), Si-O (469 cm^{-1}) and Al-O (566 cm^{-1}) decreased, showing the destruction of aluminosilicate and silicate. The absorption peak at 1424 cm^{-1} also changed, indicating dissolution of carbonate. In brief, the surface of coal fly ash was eroded by bacteria, which explains how bio-desilication influences the leaching rate of REEs.

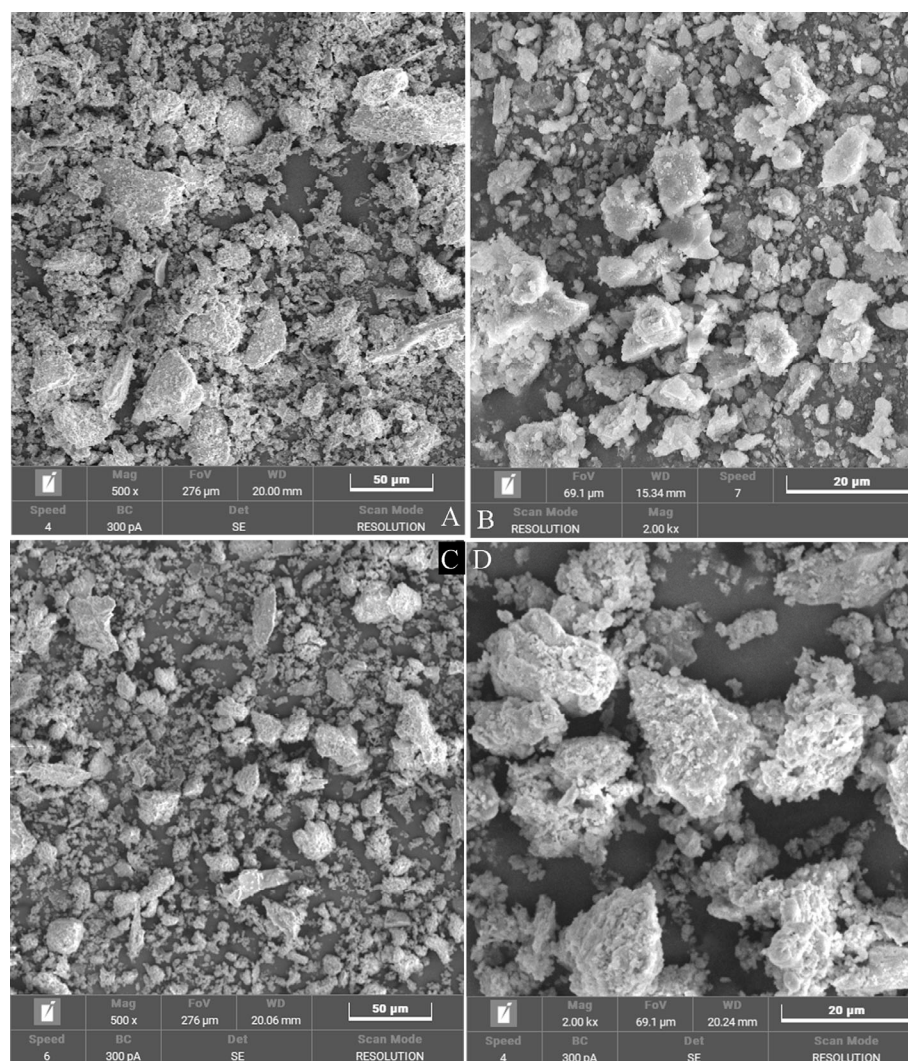


Figure 9. SEM of circulating fluidized bed coal fly ash before (A,B) and after bioleaching (C,D).

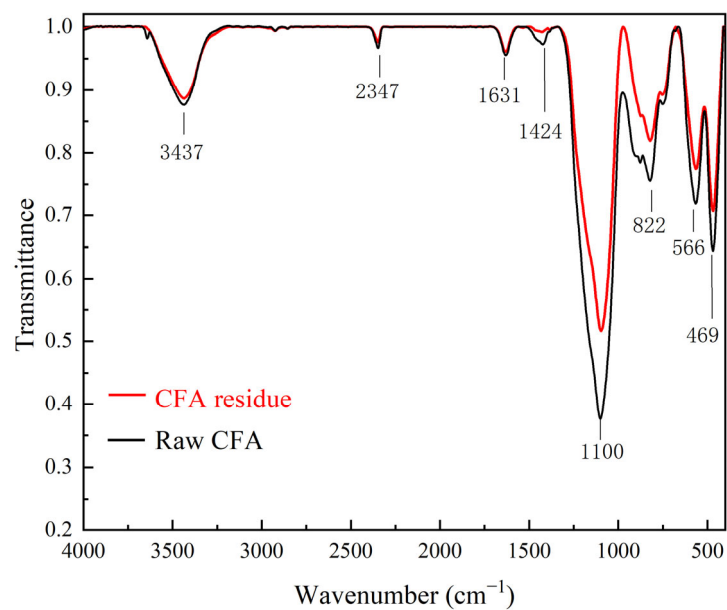


Figure 10. FTIR analyses of circulating fluidized bed coal fly ash before (raw) and after bio-desilication (residue).

Additionally, raw CFB CFA exhibited a markedly higher specific surface area than raw PCF CFA (Table 2). This is a reason why the Si and REE leaching rates of raw CFB CFA were superior to those of raw PCF CFA. The higher the specific surface area, the higher the dissolution rates of silicon [34]. The difference between the two raw coal fly ash samples in surface area is attributed to the distinct combustion method. High temperature in a pulverized coal furnace leads to the formation of spherical particles endowed with a low specific surface area. In contrast, irregular fragments are produced by CFB, which have porosity and high specific surface area. According to the adsorption and desorption curve, a greater volume of N₂ was absorbed onto raw CFB coal fly ash than onto the PCF sample. The amount of absorbed N₂ increased after bio-desilication for both samples (Figure S2). It is speculated that there were more mesopores on the surface of coal fly ash after bio-desilication, as evidenced by the pore size distribution curve (Figure S3). The average pore diameter of CFB coal fly ash was higher than that of the PCF samples, since CFB coal fly ash contained more mesopores with a pore diameter > 5 nm. Bio-desilication improved the specific surface area of both CFA samples. The specific surface area of raw CFB CFA was 9.45 m²/g, and it increased to 14.28 m²/g after bio-desilication. The surface area of PCF CFA rose from 1.88 to 8.66 m²/g after bioleaching (Table 1). Similarly, Wang et al. reported that the specific surface area of coal fly ash increased after bio-modification using *P. mucilaginosus* [36]. The specific surface area of CFA significantly affects its reactivity, and a high specific surface area favors acid penetration and dissolution of REEs. For example, Su et al. [18] reported that the particle size of coal fly ash decreased and the specific surface area increased after hydrothermal-alkali treatment, which promoted extraction of Y, La and Ce. This explained the result that the REE recovery rate was improved by bio-desilication. Moreover, the specific surface area of the CFB CFA residue was higher than that of the PCF CFA residue, in accordance with the higher REE extraction rate of the CFB CFA residue.

Table 2. Specific surface area of coal fly ash before and after bio-desilication.

Coal Fly Ash	Specific Surface Area (m ² /g)
Circulating fluidized bed, raw	9.45
Circulating fluidized bed, residue	14.28
Pulverized coal furnace, raw	1.88
Pulverized coal furnace, residue	8.66

As for mineral phases, XRD analyses revealed that there was mainly amorphous silicon in both types of coal fly ash (Figure 11). The broad hump at 2θ of 20–30° corresponds to amorphous aluminosilicate minerals, which were derived from the thermal transformation of kaolinite. PCF CFA contained more quartz and mullite than CFB CFA. Moreover, there was magnetite in PCF CFA, whereas gypsum and hematite were detected in CFB CFA. The gypsum originated from feed coal or desulfurization by calcium [43]. Pulverized coal furnace operates at a higher combustion temperature (1000–1200 °C) than circulating fluidized bed (800–900 °C). Mullite forms at high temperatures, so PCF CFA had more mullite than CFB CFA. The small amount of mullite observed in CFB CFA is probably due to the localized high-temperature combustion of small coal particles resulting from uneven temperature distribution within the circulating fluidized bed. Quartz has a high melting point (1713 °C), so quartz in feed coal remained unaltered after combustion. Fe-bearing minerals in coal gangue (e.g., pyrite) were transformed into hematite or magnetite during combustion, depending on the combustion methods [44].

After bio-desilication, the diffraction intensity of quartz and mullite decreased. Quartz has a frame structure, which is stable and very difficult to be broken down by HCl or microorganisms [45,46]. Mullite is more easily destroyed by bacteria than quartz [22]. Also, part of the dissolved Si originates from amorphous aluminosilicate. Guo et al. reported that

amorphous silicon is more easily decomposed by silicate bacterium *Bacillus amyloliquefaciens* than mullite or quartz in fly ash [23]. The activation energy of crystalline silicate is higher than that of amorphous silicate, and the dissolution rate of amorphous SiO_2 in water is ~ 10 times faster than quartz [34,47]. Some diffraction peaks of hematite disappeared in CFB after bioleaching (Figure 11A). Hematite is more readily dissolved by organic acids than magnetite. Gypsum remained intact after bio-desilication. CaCO_3 was detected in CFB CFA residue, which is from the culture medium. For PCF CFA residue, the diffraction intensity of quartz, mullite and magnetite decreased slightly (Figure 11B), indicating that a small portion of quartz was dissolved by bacteria. In summary, the low Si leaching rate of PCF CFA is attributed to its mineral phase, which contains more quartz and mullite.

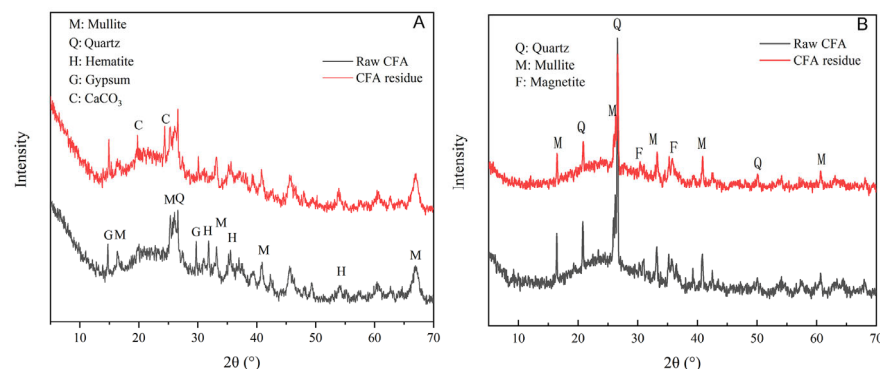


Figure 11. XRD analyses of circulating fluidized bed (A) and pulverized coal furnace (B) coal fly ash before and after bioleaching.

Overall, the bio-desilication of coal fly ash improved its REE extractability. Bacteria produced organic acids and extracellular polymeric substances, thereby creating a microenvironment conducive to the reaction of organic acids and silicate on the surface of coal fly ash. The carboxyl group attacks Si and H^+ attacks O in silicate, resulting in the cleavage of Si-O bonds. The breakage of multiple Si-O bonds enables Si dissolution in the form of silicic acid or silicate esters. Bacteria create corrosion pits on the surface, which renders the surface coarser and increases the specific surface area. With the dissolution of Si, REE carriers (e.g., REE phosphate) are exposed to react with HCl during acid leaching, thus improving REE extraction. The extent of improvement depends on the type of CFA. For circulating fluidized bed CFA, more Si was dissolved by bacteria, which leads to a substantial improvement in REE extractability. For pulverized coal furnace CFA containing larger amounts of quartz and mullite, less Si was dissolved by bacteria, which results in a slightly enhanced REE extractability. These results demonstrated the potential application of silicate bacteria in REE extraction for the first time, and the underlying mechanisms were revealed. After bio-desilication, the leachate and *P. mucilaginosus* cells can be utilized as biofertilizer in agriculture. This study provides new prospects for the comprehensive utilization of coal fly ash. In the future, longer duration bioleaching will be conducted, and the desilication ability of silicate bacteria needs to be further improved.

4. Conclusions

REEs in coal fly ash possess enormous recovery value, but direct acid leaching shows a poor extraction rate. In this study, desilication of coal fly ash was conducted with the typical silicate bacterium *P. mucilaginosus*, and the impacts of bio-desilication on REE acid leaching were explored. The main conclusions are as follows:

1. The optimal bio-desilication conditions were pulp density 1%, initial pH 7.0, initial cell concentration $OD_{600} = 0.2$ and culture medium with a nitrogen source. Organic acids were produced by *P. mucilaginosus*, which decreased pH during bio-desilication.
2. The silicon leaching rate was higher in CFB coal fly ash than in PCF coal fly ash. This is because PCF coal fly ash has a smooth surface and lower specific surface area, and contains more quartz and mullite, which are more resistant to biocorrosion compared to amorphous silicate.
3. Bio-desilication improved the REE leaching rate of coal fly ash, with an increase of 8–15% for CFB coal fly ash and only 4–5% for PCF coal fly ash, indicating that the impact of bio-desilication on REE extraction depends on the coal fly ash type.
4. *P. mucilaginosus* destroyed the structure of aluminosilicate, made the surface of CFA coarser and increased the specific surface area of CFA, which released REEs encapsulated in aluminosilicate and enhanced the reaction between coal fly ash and HCl, thus promoting REE recovery.

In the future, the desilication ability of silicate bacteria needs to be improved while lowering the cost, and bio-desilication mechanisms should be investigated further.

Supplementary Materials: The following supporting information can be downloaded at <https://www.mdpi.com/article/10.3390/met15080891/s1>, Figure S1. Acid leaching rate of total rare earth elements from CFB (A) and PCF (B) coal fly ash residue of sterile culture medium leaching. Figure S2. Adsorption and desorption curve of coal fly ash: raw CFB coal fly ash (A), CFB coal fly ash residue (B), raw PCF coal fly ash (C), PCF coal fly ash residue (D). Figure S3. Pore size distribution on surface of coal fly ash: raw CFB coal fly ash (A), CFB coal fly ash residue (B), raw PCF coal fly ash (C), PCF coal fly ash residue (D). Table S1. Main elemental composition of CFB and PCF coal fly ash samples (wt.%). Table S2. Concentration of rare earth elements in CFB and PCF coal fly ash samples (ppm).

Author Contributions: Conceptualization, S.S.; methodology, T.C.; software, T.C.; validation, S.R. and S.S.; formal analysis, S.R.; investigation, S.R.; resources, T.C. and S.S.; data curation, S.R.; writing—original draft preparation, S.S.; writing—review and editing, S.S. and J.P.; visualization, T.C. and S.S.; supervision, J.P.; project administration, J.P.; funding acquisition, S.S. and J.P. All authors have read and agreed to the published version of the manuscript.

Funding: This research was funded by the National Nature Science Foundation of China, grant numbers 52204297 and 52204292, and the interdisciplinary program between science and engineering of CUMT.

Data Availability Statement: The original contributions presented in this study are included in the article/Supplementary Materials. Further inquiries can be directed to the corresponding author.

Conflicts of Interest: The authors declare no conflicts of interest.

Abbreviations

The following abbreviations are used in this manuscript:

REEs	Rare earth elements
CFB	Circulating fluidized bed
PCF	Pulverized coal furnace
CFA	Coal fly ash
FTIR	Fourier transform infrared
XRD	X-ray diffraction
SEM	Scanning electron microscopy
HPLC	High-performance liquid chromatography
OD_{600}	Optical density at 600 nm
RSD	Relative standard deviation

References

1. Zhang, W.; Noble, A.; Yang, X.; Honaker, R. A comprehensive review of rare earth elements recovery from coal-related materials. *Minerals* **2020**, *10*, 451. [\[CrossRef\]](#)
2. Wu, G.; Wang, T.; Chen, G.; Shen, Z.; Pan, W.-P. Coal fly ash activated by NaOH roasting: Rare earth elements recovery and harmful trace elements migration. *Fuel* **2022**, *324*, 124515. [\[CrossRef\]](#)
3. Pan, J.; Zhou, C.; Tang, M.; Cao, S.; Liu, C.; Zhang, N.; Wen, M.; Luo, Y.; Hu, T.; Ji, W. Study on the modes of occurrence of rare earth elements in coal fly ash by statistics and a sequential chemical extraction procedure. *Fuel* **2019**, *237*, 555–565. [\[CrossRef\]](#)
4. Yildirim, H.; Sümer, M.; Akyüncü, V.; Gürbüz, E. Comparison on efficiency factors of F and C types of fly ashes. *Constr. Build. Mater.* **2011**, *25*, 2939–2947. [\[CrossRef\]](#)
5. Liu, P.; Huang, R.; Tang, Y. Comprehensive understandings of rare earth element (REE) Speciation in coal fly ashes and implication for REE extractability. *Environ. Sci. Technol.* **2019**, *53*, 5369–5377. [\[CrossRef\]](#) [\[PubMed\]](#)
6. Pan, J.; Long, X.; Zhang, L.; Shoppert, A.; Valeev, D.; Zhou, C.; Liu, X. The discrepancy between coal ash from muffle, circulating fluidized bed (CFB), and pulverized coal (PC) furnaces, with a focus on the recovery of iron and rare earth elements. *Materials* **2022**, *15*, 8494. [\[CrossRef\]](#) [\[PubMed\]](#)
7. Pan, J.; Nie, T.; Vaziri Hassas, B.; Rezaee, M.; Wen, Z.; Zhou, C. Recovery of rare earth elements from coal fly ash by integrated physical separation and acid leaching. *Chemosphere* **2020**, *248*, 126112. [\[CrossRef\]](#)
8. Pan, J.H.; Hassas, B.V.; Rezaee, M.; Zhou, C.C.; Pisupati, S.V. Recovery of rare earth elements from coal fly ash through sequential chemical roasting, water leaching, and acid leaching processes. *J. Clean. Prod.* **2021**, *284*, 124725. [\[CrossRef\]](#)
9. Wang, Z.; Dai, S.; Zou, J.; French, D.; Graham, I.T. Rare earth elements and yttrium in coal ash from the Luzhou power plant in Sichuan, Southwest China: Concentration, characterization and optimized extraction. *Int. J. Coal Geol.* **2019**, *203*, 1–14. [\[CrossRef\]](#)
10. Taggart, R.K.; Hower, J.C.; Hsu-Kim, H. Effects of roasting additives and leaching parameters on the extraction of rare earth elements from coal fly ash. *Int. J. Coal Geol.* **2018**, *196*, 106–114. [\[CrossRef\]](#)
11. Shi, S.; Pan, J.; Dong, B.; Zhou, W.; Zhou, C. Bioleaching of rare earth elements: Perspectives from mineral characteristics and microbial species. *Minerals* **2023**, *13*, 1186. [\[CrossRef\]](#)
12. Yang, Z.; Peng, C.; Iwan, M.; Chen, L.; He, M.; Zhang, Z.; Chen, Y.; Tang, J.; Wang, J.; Liu, Y.; et al. Microbial consortia-driven bioweathering provides new potential for sustainable recovery of rare earth elements (REE) in fly ash: From metagenome exploration to performance verification. *J. Environ. Chem. Eng.* **2024**, *12*, 113540. [\[CrossRef\]](#)
13. Shen, L.; Zhou, H.; Qiu, G.; Zhao, H. A review of bioleaching combined with low-cost fermentation and metabolic engineering technology to leach rare earth elements. *J. Environ. Chem. Eng.* **2024**, *12*, 112117. [\[CrossRef\]](#)
14. Seidel, A.; Zimmels, Y.; Armon, R. Mechanism of bioleaching of coal fly ash by *Thiobacillus thiooxidans*. *Chem. Eng. J.* **2001**, *83*, 123–130. [\[CrossRef\]](#)
15. Ma, J.; Li, S.; Wang, J.; Jiang, S.; Panchal, B.; Sun, Y. Bioleaching rare earth elements from coal fly ash by *Aspergillus niger*. *Fuel* **2023**, *354*, 129387. [\[CrossRef\]](#)
16. Fan, X.; Lv, S.; Xia, J.; Nie, Z.; Zhang, D.; Pan, X.; Liu, L.; Wen, W.; Zheng, L.; Zhao, Y. Extraction of Al and Ce from coal fly ash by biogenic Fe³⁺ and H₂SO₄. *Chem. Eng. J.* **2019**, *370*, 1407–1424. [\[CrossRef\]](#)
17. Rezaei, H.; Shafaei, S.Z.; Abdollahi, H.; Ghassa, S.; Boroumand, Z.; Fallah Nosratabad, A. Spent-medium leaching of germanium, vanadium and lithium from coal fly ash with biogenic carboxylic acids and comparison with chemical leaching. *Hydrometallurgy* **2023**, *217*, 106038. [\[CrossRef\]](#)
18. Su, H.; Tan, F.; Lin, J. An integrated approach combines hydrothermal chemical and biological treatment to enhance recycle of rare metals from coal fly ash. *Chem. Eng. J.* **2020**, *395*, 124640. [\[CrossRef\]](#)
19. Raturi, G.; Sharma, Y.; Rana, V.; Thakral, V.; Myaka, B.; Salvi, P.; Singh, M.; Dhar, H.; Deshmukh, R. Exploration of silicate solubilizing bacteria for sustainable agriculture and silicon biogeochemical cycle. *Plant Physiol. Biochem.* **2021**, *166*, 827–838. [\[CrossRef\]](#)
20. Zhang, Q.; Yan, X.; Peng, Y. Feasibility of bioleaching for extracting effective silicon from coal tailings: Optimization and modeling. *J. Environ. Chem. Eng.* **2025**, *13*, 115964. [\[CrossRef\]](#)
21. Wang, Q.; Sheng, X.-F.; He, L.-Y.; Shan, Y. Improving bio-desilication of a high silica bauxite by two highly effective silica-solubilizing bacteria. *Miner. Eng.* **2018**, *128*, 179–186. [\[CrossRef\]](#)
22. Sen, S.K.; Das, M.M.; Bandyopadhyay, P.; Dash, R.R.; Raut, S. Green process using hot spring bacterium to concentrate alumina in coal fly ash. *Ecol. Eng.* **2016**, *88*, 10–19. [\[CrossRef\]](#)
23. Guo, Y.; Teng, Q.; Yang, Z.; Sun, B.; Liu, S. Investigation on bio-desilication process of fly ash based on a self-screened strain of *Bacillus amyloliquefaciens* and its metabolites. *J. Biotechnol.* **2021**, *341*, 146–154. [\[CrossRef\]](#) [\[PubMed\]](#)
24. Li, X.; Yu, Y.; Li, Y.; Yin, Z.; Liu, X.; Lian, B. Molecular mechanism of increasing extracellular polysaccharide production of *Paenibacillus mucilaginosus* K02 by adding mineral powders. *Int. Biodeterior. Biodegrad.* **2022**, *167*, 105340. [\[CrossRef\]](#)
25. Grady, E.N.; MacDonald, J.; Liu, L.; Richman, A.; Yuan, Z.-C. Current knowledge and perspectives of *Paenibacillus*: A review. *Microb. Cell Fact.* **2016**, *15*, 203. [\[CrossRef\]](#)

26. Goswami, D.; Parmar, S.; Vaghela, H.; Dhandhukia, P.; Thakker, J.N. Describing *Paenibacillus mucilaginosus* strain N3 as an efficient plant growth promoting rhizobacteria (PGPR). *Cogent Food Agr.* **2015**, *1*, 1000714. [\[CrossRef\]](#)
27. Xu, C.; Zhao, X.; Duan, H.; Gu, W.; Zhang, D.; Wang, R.; Lu, X. Synergistic enzymatic mechanism of lepidolite leaching enhanced by a mixture of *Bacillus mucilaginosus* and *Bacillus circulans*. *Sci. Total Environ.* **2024**, *947*, 174711. [\[CrossRef\]](#)
28. Zhao, J.; Wu, W.; Zhang, X.; Zhu, M.; Tan, W. Characteristics of bio-desilication and bio-flotation of *Paenibacillus mucilaginosus* BM-4 on aluminosilicate minerals. *Int. J. Miner. Process* **2017**, *168*, 40–47. [\[CrossRef\]](#)
29. Zhang, Q.; Liang, L.; Jing, M.; Yan, X.; Peng, Y. Bioleaching of available silicon from coal tailings using *Bacillus mucilaginosus*: A sustainable solution for soil improvement. *Environ. Sci. Pollut. Res.* **2023**, *30*, 93142–93154. [\[CrossRef\]](#)
30. Hu, X.-F.; Li, S.-X.; Wu, J.-G.; Wang, J.-F.; Fang, Q.-L.; Chen, J.-S. Transfer of *Bacillus mucilaginosus* and *Bacillus edaphicus* to the genus *Paenibacillus* as *Paenibacillus mucilaginosus* comb. nov. and *Paenibacillus edaphicus* comb. nov. *Int. J. Syst. Evol. Microbiol.* **2010**, *60*, 8–14. [\[CrossRef\]](#)
31. Liu, W.; Xu, X.; Wu, X.; Yang, Q.; Luo, Y.; Christie, P. Decomposition of silicate minerals by *Bacillus mucilaginosus* in liquid culture. *Environ. Geochem. Health* **2006**, *28*, 133–140. [\[CrossRef\]](#)
32. Tian, H.; Cai, Z.; Zhang, Y.; Zheng, Q. Chemical mutation of *Bacillus mucilaginosus* genes to enhance the bioleaching of vanadium-bearing shale. *Biochem. Eng. J.* **2023**, *197*, 108962. [\[CrossRef\]](#)
33. Hong, D.F. Determination of silicon dioxide in kaolin by silicon molybdenum blue spectrophotometry. *Yejin Fenxi/Metall. Anal.* **2017**, *37*, 59–64. [\[CrossRef\]](#)
34. Ehrlich, H.; Demadis, K.D.; Pokrovsky, O.S.; Koutsoukos, P.G. Modern views on desilicification: Biosilica and abiotic silica dissolution in natural and artificial environments. *Chem. Rev.* **2010**, *110*, 4656–4689. [\[CrossRef\]](#)
35. DeliĆ, D.; Stajković-Srbinić, O.; Buntić, A. Hazards and usability of coal fly ash. In *Advances in Understanding Soil Degradation*; Saljnikov, E., Mueller, L., Lavrishchev, A., Eulenstein, F., Eds.; Springer International Publishing: Cham, Switzerland, 2022; pp. 571–608.
36. Wang, W.; Guo, S.; Gu, X.; Li, X.; Huang, W.; Li, A. Bio-modification and application of coal fly ash in cementitious composites. *Case Stud. Constr. Mat.* **2022**, *17*, e01584. [\[CrossRef\]](#)
37. Zhang, L.; Qiu, G.-Z.; Hu, Y.-H.; Sun, X.-J.; Li, J.-H.; Gu, G.-H. Bioleaching of pyrite by *A. ferrooxidans* and *L. ferriphilum*. *Trans. Nonferr. Met. Soc. China* **2008**, *18*, 1415–1420. [\[CrossRef\]](#)
38. Lin, Y.; Li, S.; Li, X.; Lin, H.; Lei, N.; Wu, D.; Tong, J.; Xie, H. Bioleaching of silicon from fly ash by co-culture of silicate bacteria and fungi. *Water Air Soil Pollut.* **2023**, *234*, 755. [\[CrossRef\]](#)
39. Li, O.; Lu, C.; Liu, A.; Zhu, L.; Wang, P.-M.; Qian, C.-D.; Jiang, X.-H.; Wu, X.-C. Optimization and characterization of polysaccharide-based bioflocculant produced by *Paenibacillus elgii* B69 and its application in wastewater treatment. *Bioresour. Technol.* **2013**, *134*, 87–93. [\[CrossRef\]](#)
40. Tang, J.; Qi, S.; Li, Z.; An, Q.; Xie, M.; Yang, B.; Wang, Y. Production, purification and application of polysaccharide-based bioflocculant by *Paenibacillus mucilaginosus*. *Carbohydr. Polym.* **2014**, *113*, 463–470. [\[CrossRef\]](#)
41. Lv, Y.; Li, J.; Chen, Z.; Liu, X.; Chen, B.; Zhang, M.; Ke, X.; Zhang, T.C. Effects of different silicate minerals on silicon activation by *Ochrobactium* sp. T-07-B. *Environ. Sci. Pollut. Res.* **2022**, *29*, 87393–87401. [\[CrossRef\]](#)
42. Liu, Y.; Tian, B.; Xiao, R.; Li, Y.; Li, Z.; Cui, L.; Li, Z.; Liang, H. The bio-activation of pozzolanic activity of circulating fluidized-bed fly ash by *Paenibacillus mucilaginosus*. *Adv. Powder Technol.* **2022**, *33*, 103621. [\[CrossRef\]](#)
43. Huang, S.; Ning, S.; Zhang, D.; Cai, Y.; Yan, X.; Liu, K.; Xu, X. Rare earth element characteristics in coal ash from the Jungar energy gangue power plant, Inner Mongolia, China. *Minerals* **2023**, *13*, 1212. [\[CrossRef\]](#)
44. Wang, T.; Yang, H.; Wu, Y.; Liu, Q.; Lv, J.; Zhang, H. Experimental study on the effects of chemical and mineral components on the attrition characteristics of coal ashes for fluidized bed boilers. *Energy Fuels* **2012**, *26*, 990–994. [\[CrossRef\]](#)
45. Chen, H.; Wen, Z.; Pan, J.; Zhang, L.; He, X.; Valeev, D.; Zhou, C. Study on leaching behavior differences of rare earth elements from coal fly ash during microwave-assisted HCl leaching. *Int. J. Coal Prep. Util.* **2023**, *43*, 1993–2015. [\[CrossRef\]](#)
46. Matias, P.C.; Mattiello, E.M.; Santos, W.O.; Badel, J.L.; Alvarez V., V.H. Solubilization of a K-silicate rock by *Acidithiobacillus thiooxidans*. *Miner. Eng.* **2019**, *132*, 69–75. [\[CrossRef\]](#)
47. Rimer, J.D.; Trofymuk, O.; Navrotsky, A.; Lobo, R.F.; Vlachos, D.G. Kinetic and thermodynamic studies of silica nanoparticle dissolution. *Chem. Mater.* **2007**, *19*, 4189–4197. [\[CrossRef\]](#)

Disclaimer/Publisher’s Note: The statements, opinions and data contained in all publications are solely those of the individual author(s) and contributor(s) and not of MDPI and/or the editor(s). MDPI and/or the editor(s) disclaim responsibility for any injury to people or property resulting from any ideas, methods, instructions or products referred to in the content.